



HHS Public Access

Author manuscript

Am J Med Genet A. Author manuscript; available in PMC 2020 June 17.

Published in final edited form as:

Am J Med Genet A. 2017 March ; 173(3): 661–666. doi:10.1002/ajmg.a.38005.

***CELSR2*, Encoding a Planar Cell Polarity Protein, Is a Putative Gene in Joubert Syndrome with Cortical Heterotopia, Microphthalmia, and Growth Hormone Deficiency**

Thierry Vilboux^{1,2}, May Christine V. Malicdan^{1,3,*}, Joseph C. Roney¹, Andrew R. Cullinane^{1,4}, Joshi Stephen¹, Deniz Yildirimli¹, Joy Bryant¹, Roxanne Fischer¹, Meghana Vemulapalli⁵, James C. Mullikin⁵, NISC Comparative Sequencing Program⁵, Peter J. Steinbach⁶, William A. Gahl^{1,3,7}, Meral Gunay-Aygun^{1,7}

¹Section of Human Biochemical Genetics, Medical Genetics Branch, National Human Genome Research Institute, National Institutes of Health, Bethesda, Maryland ²Inova Translational Medicine Institute, Falls Church, Virginia ³NIH Undiagnosed Diseases Program, Common Fund, Office of the Director, National Institutes of Health, Bethesda, Maryland ⁴Department of Anatomy, Howard University College of Medicine, Washington DC ⁵NIH Intramural Sequencing Center (NISC), National Human Genome Research Institute, National Institutes of Health, Bethesda, Maryland ⁶Center for Molecular Modeling, Center for Information Technology, National Institutes of Health, Bethesda, Maryland ⁷Office of the Clinical Director, National Human Genome Research Institute, National Institutes of Health, Bethesda, Maryland

Abstract

Joubert syndrome is a ciliopathy characterized by a specific constellation of central nervous system malformations that result in the pathognomonic “molar tooth sign” on imaging. More than 27 genes are associated with Joubert syndrome, but some patients do not have mutations in any of these genes. *Celsr1*, *Celsr2*, and *Celsr3* are the mammalian orthologues of the drosophila planar cell polarity protein, *flamingo*; they play important roles in neural development, including axon guidance, neuronal migration, and cilium polarity. Here, we report bi-allelic mutations in *CELSR2* in a Joubert patient with cortical heterotopia, microphthalmia, and growth hormone deficiency.

*Correspondence to: May Christine V. Malicdan, M.D., Ph.D., Section of Human Biochemical Genetics, Medical Genetics Branch, National Human Genome Research Institute, National Institutes of Health, 10 Center Drive, Bethesda 20892, Maryland. malicdanm@mail.nih.gov.

Conflict of interest: None.

WEB RESOURCES

ExAC Browser, <http://exac.broadinstitute.org/>

Mutation Taster: <http://www.mutationtaster.org/>

OMIM, <http://www.omim.org/>

PolyPhen-2, <http://genetics.bwh.harvard.edu/pph2/>

SIFT, <http://sift.bii.a-star.edu.sg/>

SUPPORTING INFORMATION

Additional supporting information may be found in the online version of this article at the publisher’s web-site.

Keywords

Joubert syndrome; CELSR2; planar cell polarity; ciliopathy

INTRODUCTION

Joubert syndrome (JS) comprises of a genetically and clinically heterogeneous group of ciliopathies diagnosed based on the common pathognomonic brain imaging finding called the “molar tooth sign.” This malformation is caused by a specific constellation of hindbrain and midbrain anomalies including cerebellar vermis hypoplasia. Typical clinical features of JS include hypotonia, developmental delay, and subsequent ataxia and speech apraxia. Nystagmus, strabismus, and abnormal respiratory patterns, that is, apnea and intermittent tachypnea, are common. Other variable features include retinal dystrophy, fibrocystic disease of the kidneys and liver, and polydactyly. The more than 27 JS genes identified to date do not account for all JS patients, suggesting further genetic heterogeneity [Parisi and Glass, 2003].

Celsr1, *Celsr2*, and *Celsr3* are the mammalian orthologues of flamingo, the drosophila planar cell polarity protein that belongs to a unique cadherin subfamily. *Celsr1-3* functions in neural development, specifically in axon guidance, neuronal migration, and cilium polarity [Huber and Cormier-Daire, 2012].

Here, we describe a patient with JS and cortical heterotopia, microphthalmia, severe growth retardation, growth hormone deficiency, and cone-shaped epiphyses in whom we identified bi-allelic mutations in *CELSR2*.

METHODS

Patients

Between 2003 and 2014, 103 patients with Joubert syndrome were prospectively evaluated at the National Institutes of Health (NIH) Clinical Center, under protocol 03-HG-0264, “Clinical and Molecular Investigations Into Ciliopathies” (www.clinicaltrials.gov; [NCT00068224](https://clinicaltrials.gov/ct2/show/study/NCT00068224)). This study was approved by the National Human Genome Research Institute Institutional Review Board, and written informed consent was obtained from the proband’s parents. Evaluations at the NIH Clinical Center included exome sequencing, neurocognitive testing, complete ophthalmological examination, echocardiography, abdominal ultrasonography, skeletal survey, and comprehensive blood and urine testing including evaluation of liver and kidney function as well as hormone levels.

Sequencing and Variant Analysis

For exome sequencing, we used the HiSeq2000 (Illumina) [Bentley et al., 2008] that employed 101-bp paired-end read sequencing. Image analysis and base calling were performed using Illumina Genome Analyzer Pipeline software (versions 1.13.48.0) with default parameters. Reads were aligned to a human reference sequence (UCSC assembly hg19, NCBI build 37) using a package called Efficient Large-scale Alignment of Nucleotide

Databases (Illumina). Genotypes were called at all positions where there were high-quality sequence bases using a Bayesian algorithm called the Most Probable Genotype [Teer and Mullikin, 2010] and variants were filtered using the graphical software tool VarSifter v1.5 [Teer et al., 2012]. The database dbSNP (see [URLs](#)) covers the 1.22% of the human genome corresponding to the Consensus Conserved Domain Sequences and more than 1,000 noncoding RNAs [Gnirke et al., 2009].

For dideoxy sequencing, primers were designed to amplify *CELSR2* (primer sequences available upon request). Direct sequencing of the PCR amplification products was carried out using BigDye 3.1 Terminator chemistry (Applied Biosystems) and separated on an ABI 3130xl genetic analyzer (Applied Biosystems). Data were evaluated using Sequencher v5.0 software (Gene Codes Corporation).

RESULTS

Clinical Report

The patient is an 8-year-old female (Fig. 1A and B) born at 37 week gestation via caesarean-section due to failure of labor to progress. Apgar scores were 7 and 9 at 1 and 5 min, respectively. Birth weight was 3,640 g (75th %), and length 50 cm (50th %). Head circumference was 36 cm (70th %). Nystagmus, small left eye, and left ptosis were noted at birth. Within the first hours of life, the infant developed tachypnea and apnea episodes. A diagnosis of JS was made based on brain MRI findings of a severely hypoplastic and dysplastic cerebellar vermis and the molar tooth sign (Fig. 1C and D). Other brain MRI findings included left occipital cortical heterotopia (Fig. 1E), and hypoplastic extraocular muscles (Fig. 1F). Apneas resolved after the first weeks of life but the infant continued to have panting episodes. She was able to breast feed well for the first year of life, but did not tolerate solid foods, due to difficulty swallowing, and remained on pureed foods till age 8. There was no polyuria nor polydipsia. She underwent multiple surgeries for ptosis and strabismus. She had severe global developmental delay, only beginning to walk with a walker at age 6 years. At age 8, she had no words but used some sounds and a few signs for communication.

Physical examination at the NIH at age 8 years showed a small, but well-nourished female with significant developmental delay. She was nonverbal but interacted through basic signing and noises. Height was 93.3 cm (−6.9 SD, average for 3 years), weight was 15.1 kg (−4.2 SD), and body mass index was normal at 17.3 kg/m² (75th and 85th %). Head circumference was relatively large at 52 cm (+2.5 SD for 3 years). Arm span was 91.5 cm. Upper to lower segment ratio was 1.05 (0 SD). She had a relatively large head with a tall forehead, hypoplastic supraorbital ridges, wide-spaced eyes, epicanthal folds, and borderline low set ears (Fig. 1B). The left eye was microphthalmic with severe ptosis. The palate was high and narrow with surrounding overgrowth of the gums; the uvula was normal. The girl had generalized low muscle tone and a wide-based gait. Neurodevelopmental testing was limited to structured interview with parents (Vineland Adaptive Behavior Scales-II) because patient had no reliable means of indicating a response on available standardized tests. Vineland adaptive behavior composite score was 55 ± 5, communication 54 ± 8, daily living skills 51 ± 8, socialization 57 ± 7, and motor skills: 40 ± 10; the normal means for all

categories are 100 ± 15). Within the communication domain, she turned her eyes and head toward sound and looked toward her parents when they talked to her. She was able to point to body parts and indicate more, yes, no, eat, and want reliably. She fed herself with a spoon, but could not use a pincer grasp to pick up small objects.

Bone age was significantly delayed at approximately 4 years. Skeletal survey showed a large head with increased craniofacial ratio (Fig. 1G and H). Copper beaten marks were noted in the skull (Fig. 1H). There were cone-shaped epiphysis in hands and feet (Fig. 1I and J). Serum IGF-1 level was less than 25ng/ml (Z score < -2.73); normal for Tanner I female, 49–342. The TSH was normal, the T4 was mildly elevated. There was no obvious structural anomaly of the pituitary gland on brain MRI.

Ophthalmological examination at NIH revealed bilateral restricted ocular motility, strabismus (exotropia and hypertropia), left ptosis, left microphthalmia, and bilateral myopic astigmatism. Extraocular eye movements were restricted: on the right, ductions were -2 abduction, -4 adduction, almost no elevation and depression; on the left, ductions were almost fixed. She was able to fix and follow on the right and had only light perception on the left. Retinal examination was normal except for a patch of salt and pepper pigmentary changes in the inferior periphery of the left eye. Liver and kidney related serum chemistries and abdominal ultra-sonography were normal.

Molecular Data

Exome sequencing revealed compound heterozygous variants in *CELSR2* (NM_001408.2):c.1150G>A; p.Ala384Thr and (NM_001408.2):c.6908C>T; p.Thr2303Met. The maternally inherited c.6908C>T (Fig. 2A) is known to public databases (dbSNP, rs150873094; ESP, ESP6500SIV2, MAF of 0.01%, and EXAC, MAF of 0.0025%) (see URLs). This variant results in a Threonine to Methionine change in a highly conserved residue 2303, and is predicted to be deleterious (Supplementary Table S1). The paternally inherited c.1150G>A (Fig. 2A) is known to EXAC with a total minor allele frequency (MAF) of 0.0083%. On the protein level, this results in a change of Alanine to Threonine in residue 384, which is located in the second of nine cadherin-repeat domains (Fig. 2B); this change is predicted to be damaging by pathogenicity prediction software (Supplementary Table SI). Homology modeling of the relevant *CELSR2* domains, performed using the Prime software tools (Schrodinger, LLC), indicates that the mutations A384T and T2303M both appear on the protein surface (Fig. 2C), potentially affecting protein-protein interactions in the extracellular milieu. The T2303M mutation is located in the so-called GPCR-autoproteolysis inducing (GAIN) domain [Arac et al., 2012]. This mutation is proximal to the GPCR proteolysis site (GPS) motif, with its conserved disulfide bridges. Other biallelic variants identified through whole exome analysis are listed in Supplementary Table SII.

DISCUSSION

Ciliopathies are characterized by their extreme pleiotropy; how individual defects of the same cellular organelle lead to variable involvement of multiple organs, with overlapping but distinct phenotypes remains unknown [Badano et al., 2006; Novarino et al., 2011]. To date more than 50 genes that encode cilia-related proteins are implicated in ciliopathies, some of

which overlap in clinical characteristics. In this context, the discovery of new genes associated with ciliopathy phenotypes is not surprising. The pleiotropy in ciliopathies nonetheless makes studies on genotype-phenotype correlation difficult and often limited.

In this report, we identified biallelic mutations in *CELSR2* that might be associated with this patient's phenotype. *Celsr1*, *Celsr2*, and *Celsr3* are widely expressed in the nervous system, functioning in axon guidance, neuronal migration, and cilium polarity [Formstone and Little, 2001]. In mice, *Celsr2* is expressed in all brain areas [Formstone and Little, 2001; Tissir et al., 2010] and it regulates dendritic maintenance and growth. Mice with homozygous null mutations in *Celsr2* develop hydrocephalus due to decreased numbers of ependymal cilia that are also short and abnormally oriented [Tissir et al., 2010]. Furthermore, the lateral plasma membrane localization of the two planar cell polarity proteins, *Vangl2* and *Frizzled3*, is disrupted in ependymal cell precursors in *Celsr2*-mutant mice, providing evidence that *Celsr2* regulates ciliogenesis through PCP signaling [Tissir et al., 2010]. Abnormalities of planar cell polarity have been shown in many ciliopathies including Bardet-Biedl syndrome [Ross et al., 2005], oral facial digital syndrome type I [Ferrante et al., 2009], and polycystic kidney disease [Ohata et al., 2015]. In addition, mice with defective *mksl*, a ciliary protein defective in Meckel-Gruber and Bardet-Biedl syndromes, show features indicating disruption of planar cell polarity [Cui et al., 2011]. Hence, our patient's structural brain anomalies, central nervous system dysfunction, and severe global developmental delay might be associated with a defect in *CELSR2* function. Discovery of other cases with mutations in the same gene will strengthen the association of *CELSR2* with ciliopathy. The authors, however, were unable to identify cases with similar phenotype and genotype in available collaborators and resources.

Growth hormone deficiency occurs in a small number of patients with JS [Parisi and Glass, 2003]. We screened our patient for additional pituitary hormone deficiencies including central hypothyroidism, adrenal insufficiency, diabetes insipidus, and central hypogonadism. Thyroid function tests showed a normal TSH with a mildly elevated free T4, which was not consistent with central hypothyroidism. Antidiuretic hormone deficiency was unlikely as she did not have polyuria or polydipsia. Testing for luteinizing hormone and follicle stimulating hormone deficiencies was difficult; the patient was too young to manifest absent, delayed, or incomplete pubertal development. She had no clinical signs of adrenal insufficiency such as vomiting or weight loss, and had undergone multiple surgeries with no adrenal crises, so we consider her unlikely to have adrenocorticotropic hormone deficiency. Our patient's severe growth retardation was probably due to the combined effect of growth hormone deficiency and limited growth potential of her bones as evidenced by her abnormal epiphysis. Cone-shaped epiphyses are seen in many other skeletal ciliopathies such as Jeune syndrome and other types of short-rib polydactyly syndromes with short stature due to primary bone involvement [Huber and Cormier-Daire, 2012]. Even though our patient was not diagnosed with hydrocephalus and ventricular enlargement, her skull X-ray showed coper-beaten marks suggesting increased intracranial pressure.

The other biallelic variants we identified on exome sequencing were deemed unlikely candidates; they included NM_031935.2 (*HMCN1*), NM_001308120.1 (*FAM179B*), NM_001024858.2 (*SPTB*), and NM_006267.4 (*RANBP2*) (Supplementary Table II).

Hemicentrin-1, encoded by *HMCN1*, is a large extracellular membrane protein of the immunoglobulin superfamily that is thought to provide mechanosensory anchorage of neurons to the epidermis; monoallelic *HMCN1* variants are associated with age-related macular degeneration (ARMD1, MIM603075), which the parents and grandparents of our patient did not have. *FAMI79B* shRNA knockdown experiments showed that deficiency of this protein is not associated with satellite formation, cilia abnormalities, centriole duplication, or any other detectable ciliopathy phenotype [Gupta et al., 2015]. *SPTB* codes for erythrocytic beta spectrin; monoallelic mutations in *SPTB* are associated with Spherocytosis, type 2 (MIM 616649), which the parents do not have; in addition, biallelic *SPTB* mutations cause severe type 2 spherocytosis, which our proband does not have. *RANBP2* encodes a component of the nuclear pore complex and functions in protein export and import, protein sumoylation, and intracellular trafficking [Neilson et al., 2009]. Monoallelic variants in *RANBP2* are associated with AD acute infection-induced encephalopathy type 3 (MIM 608033); our patient's family history was negative for this disorder.

In summary, this JS patient with bi-allelic mutations in *CELSR2* potentially represents the first human ciliopathy patient described with a defect in this planar cell polarity protein. Future description of other patients with mutations in *CELSR2* and the study of their underlying cell biology will determine if a defect in *CELSR2* is causative of JS and could define new mechanisms on the role of planar cell polarity in ciliary biogenesis, positioning, and orientation.

Supplementary Material

Refer to Web version on PubMed Central for supplementary material.

ACKNOWLEDGMENTS

The authors thank the Joubert syndrome and Related Disorders Foundation for their extensive support and the patients and their families who generously participated in this investigation.

Grant sponsor: Intramural Research Program of the National Human Genome Research Institute; Grant sponsor: Center for Information Technology, National Institutes of Health.

REFERENCES

- Arac D, Boucard AA, Bolliger MF, Nguyen J, Soltis SM, Sudhof TC, Brunger AT. 2012 A novel evolutionarily conserved domain of cell-adhesion GPCRs mediates autoproteolysis. *EMBO J* 31:1364–1378. [PubMed: 22333914]
- Badano JL, Mitsuma N, Beales PL, Katsanis N. 2006 The ciliopathies: An emerging class of human genetic disorders. *Annu Rev Genomics Hum Genet* 7:125–148. [PubMed: 16722803]
- Bentley DR, Balasubramanian S, Swerdlow HP, Smith GP, Milton J, Brown CG, Hall KP, Evers DJ, Barnes CL, Bignell HR, Boutell JM, Bryant J, Carter RJ, Keira Cheatham R, Cox AJ, Ellis DJ, Flatbush MR, Gormley NA, Humphray SJ, Irving LJ, Karbelashvili MS, Kirk SM, Li H, Liu X, Maisinger KS, Murray LJ, Obradovic B, Ost T, Parkinson ML, Pratt MR, Rasolonjatovo IM, Reed MT, Rigatti R, Rodighiero C, Ross MT, Sabot A, Sankar SV, Scally A, Schroth GP, Smith ME, Smith VP, Spiridou A, Torrance PE, Tzonev SS, Vermaas EH, Walter K, Wu X, Zhang L, Alam MD, Anastasi C, Aniebo IC, Bailey DM, Bancarz IR, Banerjee S, Barbour SG, Baybayan PA, Benoit VA, Benson KF, Bevis C, Black PJ, Boodhun A, Brennan JS, Bridgham JA, Brown RC, Brown AA, Buermann DH, Bundu AA, Burrows JC, Carter NP, Castillo N, Chiara ECM, Chang S,

- Neil Cooley R, Crake NR, Dada OO, Diakoumakos KD, Dominguez-Fernandez B, Earnshaw DJ, Egbujor UC, Elmore DW, Etchin SS, Ewan MR, Fedurco M, Fraser LJ, Fuentes Fajardo KV, Scott Furey W, George D, Gietzen KJ, Goddard CP, Golda GS, Granieri PA, Green DE, Gustafson DL, Hansen NF, Harnish K, Haudenschild CD, Heyer NI, Hims MM, Ho JT, Horgan AM, Hoschler K, Hurwitz S, Ivanov DV, Johnson MQ, James T, Huw Jones TA, Kang GD, Kerelska TH, Kersey AD, Khrebtukova I, Kindwall AP, Kingsbury Z, Kokko-Gonzales PI, Kumar A, Laurent MA, Lawley CT, Lee SE, Lee X, Liao AK, Loch JA, Lok M, Luo S, Mammen RM, Martin JW, McCauley PG, McNitt P, Mehta P, Moon KW, Mullens JW, Newington T, Ning Z, Ling Ng B, Novo SM, O'Neill MJ, Osborne MA, Osnowski A, Ostadan O, Paraschos LL, Pickering L, Pike AC, Chris Pinkard D, Pliskin DP, Podhasky J, Quijano VJ, Raczky C, Rae VH, Rawlings SR, Chiva Rodriguez A, Roe PM, Rogers J, Rogert Bacigalupo MC, Romanov N, Romieu A, Roth RK, Rourke NJ, Ruediger ST, Rusman E, Sanches-Kuiper RM, Schenker MR, Seoane JM, Shaw RJ, Shiver MK, Short SW, Sizto NL, Sluis JP, Smith MA, Ernest Sohna Sohna J, Spence EJ, Stevens K, Sutton N, Szajkowski L, Tregidgo CL, Turcatti G, Vandevondele S, Verhovsky Y, Virk SM, Wakelin S, Walcott GC, Wang J, Worsley GJ, Yan J, Yau L, Zuerlein M, Mullikin JC, Hurles ME, McCooke NJ, West JS, Oaks FL, Lundberg PL, Klenerman D, Durbin R, Smith AJ. 2008 Accurate whole human genome sequencing using reversible terminator chemistry. *Nature* 456:53–59. [PubMed: 18987734]
- Cui C, Chatterjee B, Francis D, Yu Q, SanAgustin JT, Francis R, Tansey T, Henry C, Wang B, Lemley B, Pazour GJ, Lo CW. 2011 Disruption of Mks1 localization to the mother centriole causes cilia defects and developmental malformations in Meckel-Gruber syndrome. *Dis Model Mech* 4:43–56. [PubMed: 21045211]
- Ferrante MI, Romio L, Castro S, Collins JE, Goulding DA, Stemple DL, Woolf AS, Wilson SW. 2009 Convergent extension movements and ciliary function are mediated by ofdl, a zebrafish orthologue of the human oral-facial-digital type 1 syndrome gene. *Hum Mol Genet* 18:289–303. [PubMed: 18971206]
- Formstone CJ, Little PF. 2001 The flamingo-related mouse Celsr family (Celsr1–3) genes exhibit distinct patterns of expression during embryonic development. *Mech Dev* 109:91–94. [PubMed: 11677057]
- Gnrke A, Melnikov A, Maguire J, Rogov P, LeProust EM, Brockman W, Fennell T, Giannoukos G, Fisher S, Russ C, Gabriel S, Jaffe DB, Lander ES, Nusbaum C. 2009 Solution hybrid selection with ultra-long oligonucleotides for massively parallel targeted sequencing. *Nat Biotechnol* 27:182–189. [PubMed: 19182786]
- Gupta GD, Coyaud E, Goncalves J, Mojarad BA, Liu Y, Wu Q, Gheiratmand L, Comartin D, Tkach JM, Cheung SW, Bashkurov M, Hasegan M, Knight JD, Lin ZY, Schueler M, Hildebrandt F, Moffat J, Gingras AC, Raught B, Pelletier L. 2015 A dynamic protein interaction landscape of the human centrosome-cilium interface. *Cell* 163:1484–1499. [PubMed: 26638075]
- Harrison OJ, Jin X, Hong S, Bahna F, Ahlsen G, Brasch J, Wu Y, Vendome J, Felsovalyi K, Hampton CM, Troyanovsky RB, Ben-Shaul A, Frank J, Troyanovsky SM, Shapiro L, Honig B. 2011 The extracellular architecture of adherens junctions revealed by crystal structures of type I cadherins. *Structure* 19:244–256. [PubMed: 21300292]
- Huber C, Cormier-Daire V. 2012 Ciliary disorder of the skeleton. *Am J Med Genet C Semin Med Genet* 160C:165–174. [PubMed: 22791528]
- Kraulis PJ. 1991 Molscript—A program to produce both detailed and schematic plots of protein structures. *J Appl Crystallogr* 24:946–950.
- Merritt EA, Bacon DJ. 1997 Raster3D: Photorealistic molecular graphics. *Method Enzymol* 277:505–524.
- Neilson DE, Adams MD, Orr CM, Schelling DK, Eiben RM, Kerr DS, Anderson J, Bassuk AG, Bye AM, Childs AM, Clarke A, Crow YJ, Di Rocco M, Dohna-Schwake C, Dueckers G, Fasano AE, Gika AD, Gionnis D, Gorman MP, Grattan-Smith PJ, Hackenberg A, Kuster A, Lentschig MG, Lopez-Laso E, Marco EJ, Mastroyianni S, Perrier J, Schmitt-Mechelke T, Servidei S, Skardoutsou A, Uldall P, van der Knaap MS, Goglin KC, Tefft DL, Aubin C, de Jager P, Hafler D, Warman ML. 2009 Infection-triggered familial or recurrent cases of acute necrotizing encephalopathy caused by mutations in a component of the nuclear pore, RANBP2. *Am J Hum Genet* 84:44–51. [PubMed: 19118815]

- Novarino G, Akizu N, Gleeson JG. 2011 Modeling human disease in humans: The ciliopathies. *Cell* 147:70–79. [PubMed: 21962508]
- Ohata S, Herranz-Perez V, Nakatani J, Boletta A, Garcia-Verdugo JM, Alvarez-Buylla A. 2015 Mechanosensory genes Pkd1 and Pkd2 contribute to the planar polarization of brain ventricular epithelium. *J Neurosci* 35:11153–11168. [PubMed: 26245976]
- Parisi M, Glass I. 2003 In: Pagon RA, Adam MP, Ardinger HH, Bird TD, Dolan CR, Fong CT, Smith RJH, Stephanie K, editors. Joubert syndrome and related disorders. Seattle (WA): GeneReviews(R) [Internet].
- Ross AJ, May-Simera H, Eichers ER, Kai M, Hill J, Jagger DJ, Leitch CC, Chapple JP, Munro PM, Fisher S, Tan PL, Phillips HM, Leroux MR, Henderson DJ, Murdoch JN, Copp AJ, Eliot MM, Lupski JR, Kemp DT, Dollfus H, Tada M, Katsanis N, Forge A, Beales PL. 2005 Disruption of Bardet-Biedl syndrome ciliary proteins perturbs planar cell polarity in vertebrates. *Nat Genet* 37:1135–1140. [PubMed: 16170314]
- Teer JK, Green ED, Mullikin JC, Biesecker LG. 2012 VarSifter: Visualizing and analyzing exome-scale sequence variation data on a desktop computer. *Bioinformatics* 28:599–600. [PubMed: 22210868]
- Teer JK, Mullikin JC. 2010 Exome sequencing: The sweet spot before whole genomes. *Hum Mol Genet* 19:R145–R151. [PubMed: 20705737]
- Tissir F, Qu Y, Montcouquiol M, Zhou L, Komatsu K, Shi D, Fujimori T, Labeau J, Tyteca D, Courtoy P, Poumay Y, Uemura T, Goffinet AM. 2010 Lack of cadherins Celsr2 and Celsr3 impairs ependymal ciliogenesis, leading to fatal hydrocephalus. *Nat Neurosci* 13:700–707. [PubMed: 20473291]



FIG. 1.

Clinical photographs and images of the patient. (A) Patient had severe growth retardation associated with relative macrocephaly. (B) Craniofacial features included tall forehead, widely spaced eyes, epicanthal folds, severe ptosis of left eye, and borderline low set ears. Brain MRI at 2 months showed molar tooth sign (circle) (C) in comparison to normal (D), left occipital cortical heterotopia (circle) (E), and hypoplastic extraocular muscles (F). Skull X-rays showed a large head with increased craniofacial ratio, copper beaten marks, and frontal bossing (G and H). Abnormal cone-shaped epiphyses were noted in hand (I) and feet (J) X-rays.

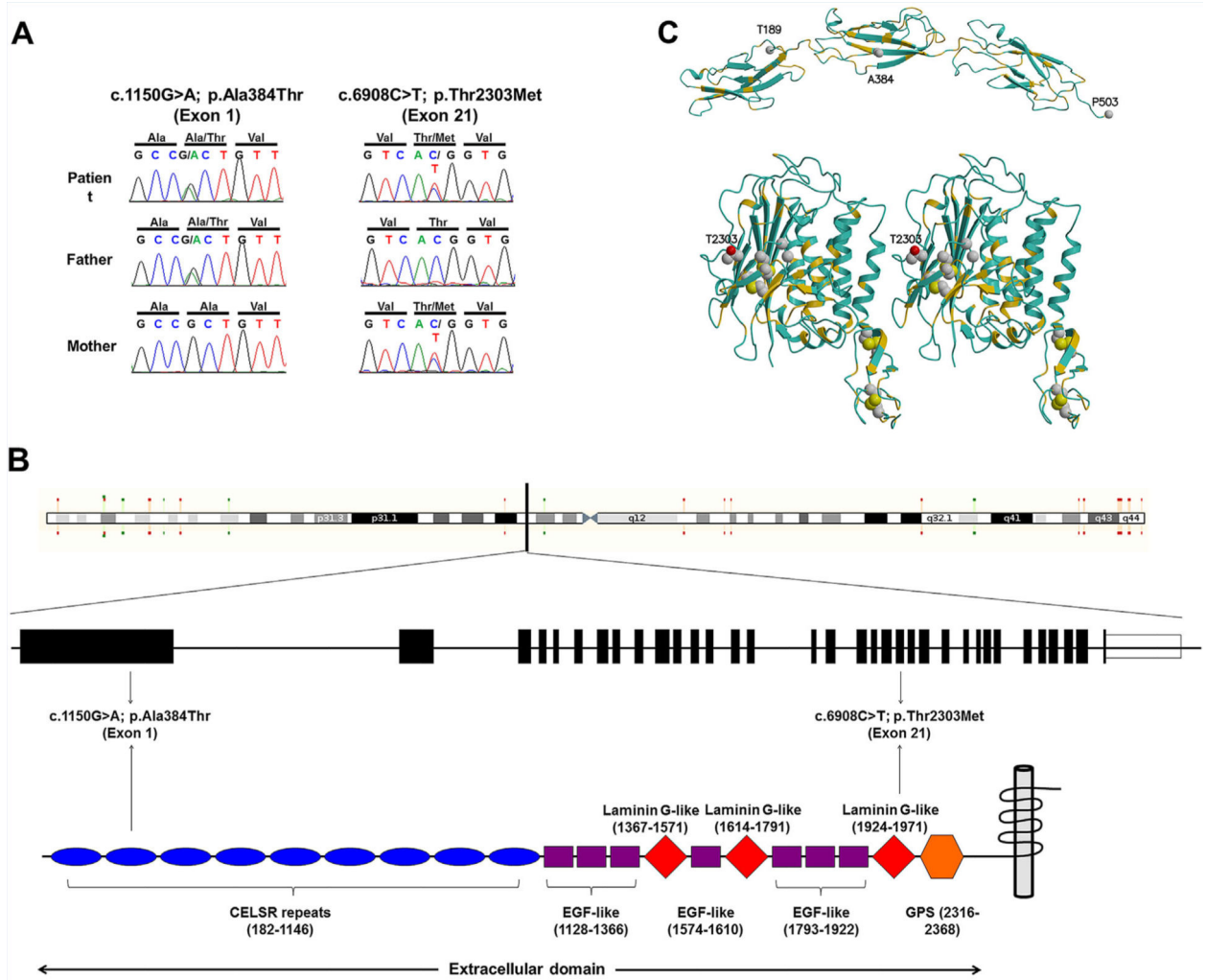


FIG. 2.

Molecular data.(A) DNA sequences showing *CELSR2* sequences of patient and her parents. Patient (upper panel) was compound heterozygote for NM_001408.2(*CELSR2*):c.1150G>A; p.Ala384Thr (inherited from the father) in exon 1 and NM_001408.2(*CELSR2*):c.6908C>T; p.Thr2303Met (inherited from the mother) in exon 21. (B) A schema showing the *CELSR2* gene and its corresponding protein with several protein domains. The mutations are located in the *CELSR* domain and laminin G-like domain, both of which are in the extracellular area. (C) Homology models of *CELSR2* domains. The first three cadherin repeats (upper) and a stereo view of the so-called HormR and GAIN domains (lower) of *CELSR2*, colored according to sequence identity with the known template structures, 3q2w.pdb [Harrison et al., 2011] and 4dlo.pdb [Arac et al., 2012], respectively. The main chain is colored gold where the template and *CELSR2* sequences are identical, blue where they differ. Note the conservation in the protein core, for example, the conserved inner faces of alpha helices. The sites of the mutations are shown as space-filling, along with the four conserved disulfide bridges (lower). The two α -carbon atoms corresponding to the cleavage site in the template structure of the brain-specific angiogenesis inhibitor 3 [Arac et al., 2012] are shown as spheres, not far from the conserved disulfide bridges of the GPS domain and the T2303M

mutation. The modeled structures were rendered using MolScript [Kraulis, 1991] and Raster3D [Merritt and Bacon, 1997].

Author Manuscript

Author Manuscript

Author Manuscript

Author Manuscript